Applied Biochemistry and Biotechnology (2024) 196:182–202
https://doi.org/10.1007/s12010-023-04507-9

ORIGINAL ARTICLE

Nimbolide Exhibits Potent Anticancer Activity Through ROS-Mediated ER Stress and DNA Damage in Human Non-small Cell Lung Cancer Cells

Xi Chen[1] · Hangshuo Zhang[2] · Yuzhu Pan[2] · Ning Zhu[3] · Lisha Zhou[4] · Guang Chen[1] · Jiabing Wang[3]

Accepted: 11 April 2023 / Published online: 27 April 2023

Abstract

The non-small cell lung cancer (NSCLC) accounts for about 85% of all lung cancers. It is usually diagnosed at an advanced stage with poor prognosis. Nimbolide (NB), a terpenoid limonoid isolated from the flowers and leaves of neem tree, possesses anticancer properties in various cancer cell lines. However, the underlying mechanism of its anticancer effect on human NSCLC cells remains unclear. In the present study, we investigated the effect of NB on A549 human NSCLC cells. We found that NB treatment inhibits A549 cells colony formation in a dose-dependent manner. Mechanistically, NB treatment increases cellular reactive oxygen species (ROS) level, leading to endoplasmic reticulum (ER) stress, DNA damage, and eventually induction of apoptosis in NSCLC cells. Furthermore, all these effects of NB were blocked by pretreatment with antioxidant glutathione (GSH), the specific ROS inhibitor. We further knockdown CHOP protein by siRNA markedly reduced NB-induced apoptosis in A549 cells. Taken together, our findings reveal that NB is an inducer of ER stress and ROS; these findings may contribute to increasing the therapeutic efficiency of NSCLC.

Keywords Nimbolide · ROS · ER stress · DNA damage · NSCLC

Xi Chen, Hangshuo Zhang, and Yuzhu Pan contribute equally to this work.

✉ Xi Chen
chenxi9212@163.com

✉ Jiabing Wang
wangjiabing9205@163.com

[1] Department of Pharmacology, School of Medicine, Taizhou University, Jiaojiang, Taizhou 318000, Zhejiang, China

[2] Department of Clinical Medicine, School of Medicine, Taizhou University, Jiaojiang, Taizhou 318000, Zhejiang, China

[3] Municipal Hospital Affiliated to Taizhou University, Jiaojiang, Taizhou 318000, Zhejiang, China

[4] Department of Biochemistry, School of Medicine, Taizhou University, Jiaojiang, Taizhou 318000, Zhejiang, China

Abbreviations

53BP1	Tumor protein p53 binding protein 1
ATF4	Activating transcription factor 4
Bax	Bcl2-associated protein x
Bcl2	B-cell lymphoma 2
DCFH-DA	2′,7′-Dichlorodihydrofluorescein diacetate
DSB	Double-strand break
EGFR	Epidermal growth factor receptor
ER	Endoplasmic reticulum
FITC	Fluorescein isothiocyanate
GSH	Glutathione
HRP	Horseradish peroxidase
MTT	3-(4,5-Dimethylthiazol-2-yl)-2,5-diphenyltetrazolium bromide
NB	Nimbolide
NSCLC	Non-small cell lung cancer
PI	Propidium iodide
ROS	Reactive oxygen species
STAT3	Signal transducer and activator of transcription 3

Introduction

Lung cancer has become the most frequent cause of cancer-related death worldwide [1]. Clinically, malignant lung tumors can be classified as small or non-small cell lung carcinomas (SCLCs and NSCLCs). In particular, 85% of lung cancer diagnoses are caused by non-small cell lung cancer (NSCLC) [2, 3]. The majority of NSCLC patients are diagnosed at advanced stages of the disease, at which stage the disease is largely incurable. Although the conventional treatment modalities such as surgery, chemotherapy, and radiotherapy have reached a great breakthrough, the 5-year survival rate for NSCLC patients remains dissatisfactory [4, 5]. In the last several years, targeted cancer therapies have showed significant clinical effects especially in NSCLC patients. NSCLC patients with epidermal growth factor receptor (EGFR) mutations have successfully been treated with EGFR tyrosine kinase inhibitors, such as erlotinib, gefitinib, and osimertinib [6–9]. However, most patients who initially responded distinctly to treatment eventually acquired resistance after about 9–14 months of treatment [10–12], which caused serious clinical problems. Thus, new therapeutic agents are urgently needed to treat and improve the NSCLC patient outcome.

Reactive oxygen species (ROS) are a family of molecules. It is formed with incomplete reduction of oxygen, including hydrogen peroxide (H_2O_2), superoxide anion ($O^{2\bullet-}$), and hydroxyl radicals (•OH) [13]. A moderate increase of ROS levels promotes cell proliferation under normal physiological conditions [14]. However, a high level of ROS can cause permanent damage to cells, resulting in apoptosis and cell cycle arrest [15]. Hence, agents manipulating ROS levels in cancer cells may be a promising strategy to target cancer cells while minimizing toxicity to normal cells.

Over the years, natural products have played a crucial role in the development of anticancer drugs [16]. Nimbolide (NB), an extractive produced from *Azadirachta indica*, consists of a terpenoid limonoid skeleton with a δ-lactone ring and an α,β-unsaturated ketone system. Previous studies have demonstrated that NB exhibit strong

pharmacological function such as anti-inflammatory [17], anti-tumor [18, 19], and antibacterial [20]. NB dose-dependently suppressed invasion and metastasis via manipulation of ERK1/2 signaling and DUSP4 expression in NSCLC cells [21]. Additionally, anticancer effect of NB has been reported in various tumor types such as breast cancer, colorectal cancer, prostate cancer, and liver cancer [19, 22–24]. Through increasing ROS levels and inhibiting signal transducer and activator of transcription 3 (STAT3) activation cascade, NB can effectively inhibit prostate cancer growth [19]. Furthermore, NB also can kill the autophagy-mediated apoptotic cell to inhibit cell proliferation thus influence breast cancer progress [25]. It also has function to reduce CD44 positive cell population and to induce mitochondrial apoptosis in pancreatic cancer cells [26]. Besides, NB also plays a crucial role in triggering endoplasmic reticulum (ER) stress to inhibit the development of specific cancer [27].

In our present study, the anticancer effects and the underlying mechanism of NB on human NSCLC cells were investigated. It was demonstrated that NB induces apoptosis in a dose-dependent manner, which is regulated by the ER stress activation through a ROS-dependent mechanism. Furthermore, NB dose-dependently increased DNA damage. Furthermore, blocking ROS production using glutathione (GSH) could totally reverse the anticancer effects of NB. Taken together, our results show that NB is an effective therapeutic candidate for NSCLC patient treatment and discover a novel mechanism of NB in anticancer activities.

Materials and Methods

Cell Culture

Human NSCLC cell lines A549 and H1650 and normal human liver cell L02 were obtained from Shanghai Institute of Biosciences and Cell Resources Center (Chinese Academy of Sciences, Shanghai, People's Republic of China). All the cells were cultured in Roswell Park Memorial Institute-1640 (RPMI-1640) medium (Thermo Fisher Scientific, Waltham, MA, USA) with 10% fetal bovine serum (FBS) and 1% antibiotic (penicillin/streptomycin) solution (Thermo Fisher Scientific). Cells were cultured in a humidified cell incubator with an atmosphere of 5% CO_2 at 37 °C.

Reagents

Nimbolide (NB) was obtained from TargetMol (Boston, USA). The compound NB was dissolved in DMSO. Antibodies including anti-Bcl-2, anti-Bax, anti-GAPDH, and horseradish peroxidase (HRP)-conjugated secondary antibodies were purchased from Santa Cruz Biotechnology (Santa Cruz, CA). Antibodies including ATF4, EIF2α, p-EIF2α, CHOP, cleaved PARP, and cleaved caspase-3 were obtained from Cell Signaling Technology (Danvers, MA). Glutathione (GSH), dimethylsulfoxide (DMSO), and methyl thiazolyl tetrazolium (MTT) were purchased from Sigma-Aldrich (St. Louis, MO). Fluorescein isothiocyanate (FITC) Annexin V Apoptosis Detection Kit and propidium iodide (PI) were purchased from BD Pharmingen (Franklin Lakes, NJ). Reactive oxygen species probe 2′,7′-dichlorodihydro fluorescein diacetate (DCFH-DA) was purchased from Thermo Fisher (Carlsbad, CA, USA). A protease phosphatase inhibitor mixture was obtained from Applygen Technologies (Beijing, People's Republic of China).

Cell Viability Assay

To measure viability of cells following NB treatment, cells (6×10^3 cells/well) were plated in 96-well plates and allowed to attach overnight in complete growth medium. NB was dissolved in DMSO and diluted with RPMI-1640 medium to obtain final concentrations of 0.5, 1, 2.5, 5, 10, and 20 μM. The NSCLC cells and normal cells were incubated with NB for 24 h or 48 h before performing the MTT assay.

Colony Formation Assay

To determine long-term effects, the cells were cultured at 500 cells/well in six-well plate with RPMI-1640 medium and allowed to attach overnight. The cells were then exposed to NB for 24 h. Following NB treatment, medium was routinely changed to fresh medium and cells were allowed to grow for 12 days until the colonies were visible. Then, colonies were fixed and stained with 2% crystal violet in ethanol. A colony is defined as a cluster of at least 50 cells that can often only be determined microscopically.

Cell Apoptosis Analysis

Cell apoptosis analysis was performed as described previously [28]. Briefly, cells were plated in six-well plates, allowed at attach overnight, and then treated with indicated concentrations of NB for 24 h in the presence or absence of 5 mM GSH pretreatment for 2 h. Cells were harvested and washed with ice-cold PBS (twice). The washed cell samples were resuspended in 500 μL binding buffer, and double stained with Annexin V-FITC and propidium iodide (PI) for 10 min. Apoptosis was analyzed by using Accuri C6 plus flow cytometer (BD Biosciences, CA, USA).

Measurement of Reactive Oxygen Species Generation

Intracellular ROS contents were assessed by flow cytometry using DCFH-DA probe. Briefly, cells were plated in six-well plates and allowed to attach overnight. Cells were then treated with indicated concentrations of NB for 3 h in presence and absence of 5 mM GSH pretreatment for 2 h. After treatment, cells were harvested and incubated with 10 μM DCFH-DA for 20 min at 37 °C in the dark. Then, the cells were washed with PBS (twice) and analyzed the mean fluorescence intensity immediately using Accuri C6 plus flow cytometry (BD Biosciences, CA, USA).

Immunofluorescence (IF) Assay

The cells were grown on a coverslip and were treated with NB (1, 2.5, 5 μM) for 20 h with or without 5 mM GSH pretreatment for 2 h. After being fixed in 4% paraformaldehyde for 10 min, cells were incubated in a permeabilization solution at room temperature for 20 min. After three times of washing with PBS, the coverslips were incubated with blocking solution for 1 h. 53BP1 (1:500 in blocking solution) was added; then, cells were incubated overnight at 4 °C. Cells were washed with blocking solution and then incubated with blocking solution including DyLight 488-conjugated secondary antibody (1:2000) for 1 h at 37 °C.

Finally, the coverslip was washed with PBST for three times and mounted with DAPI stain. Cell fluorescence was detected and imaged using Leica fluorescence microscope.

Comet Assay

DNA damage response was detected by a comet assay [29]. Briefly, cells were plated in 6-well plates and allowed to attach overnight. Cells were treated with indicated concentrations of NB for 20 h in the presence or absence of 5 mM GSH pretreatment for 2 h. After treatment, cells were harvested and washed twice with ice-cold PBS. Cells were mixed with 0.5% low-melting-temperature agarose and then transferred to slides that were coated with 1.5% normal agarose. To perform the alkaline assay, the slides were lysed in 1% Triton X-100, 10 mmol L^{-1} Tris (pH 10.0), 100 mmol L^{-1} EDTA, 2.5 M NaCl overnight at 4 °C, followed by electrophoresis in 300 mM NaOH, and 1 mmol L^{-1} EDTA at 2 V/cm for 15 min. The slides washed with water, dried with ethanol, and mounted with PI solution (20 μg/mL). Finally, the slides were captured using a fluorescence microscope (Nikon Japan). The % tail DNA and tail intensity were evaluated by CASP software.

Western Blot Analysis

Proteins from the mitochondrial, nuclear, and cytosolic fraction were prepared using lysis buffer. Protein concentrations were determined using Bradford reagent (Bio-Rad Laboratories Inc., Hercules, CA, USA) and aliquots normalized to equal quantities before loading. Protein samples were separated by SDS-PAGE. After electrophoresis, proteins were electro-transferred to poly-vinylidene difluoride (PVDF) membranes (Bio-Rad) overnight at 30 V, 4 °C. The membranes were blocked with blocking buffer (10 mM Tris–HCl, 150 mM NaCl, 0.1% Tween-20) containing 5% milk for 1 h and then incubated with respective primary antibodies for 24 h at 4 °C. Primary antibodies include anti-Bcl-2 (1:200), anti-Bax (1:200), anti-GAPDH (1:200), anti-ATF4 (1:1000), anti-EIF2α (1:1000), anti-p-EIF2α (1:1000), anti-CHOP (1:1000), anti-pro-caspase-3 (1:1000), anti-cleaved-caspase-3 (1:1000), and anti-γH2AX (1:1000). Following three washes with TBST, the blots were incubated with HRP-conjugated secondary antibodies (1:10,000) for 1 h. After additional washing with TBST, protein bands were detected by using enhanced chemiluminescence reagent (ECL kit, Amersham Biosciences). The density of the immunoreactive bands was analyzed using ImageJ software (National Institute of Health, MD).

Quantitative RT-PCR

RT-PCR assay was performed as described previously [30]. Cells were treated with NB for 3 h or 8 h; Isol-RNA Lysis Reagent (5 PRIME) was used to extract total RNA. A Bio-Rad iScript cDNA synthesis kit (500 ng total RNA) was used to generate first-strand cDNA. We used a Human Unfolded Protein Response RT2 Profiler PCR Array System (PAHS-089Z; SABiosciences) to perform real-time quantitative PCR. Real-time PCR was performed using iCycler iQ (Bio-Rad). Analysis of the data was carried out using online tools according to the manufacturer. Gene-specific primer pairs were used as follows:

CHOP-F: ATGGCAGCTGAGTCATTGCCTTTC
CHOP-R: AGAAGCAGGGTCAAGAGTGGTGAA

ATF4-F: CAGCAGCACCAGGCTCT
ATF4-R: TCGAAGGTGTCTTTGTCGGT
GAPDH-F: ACCACAGTCCATGCCATCAC
GAPDH-R: TCCACCACCCTGTTGCTGTA

Analyses were performed using a comparative threshold cycle method based on GAPDH as a housekeeping gene.

Transient Transfection of Small Interfering RNA (siRNA)

To knockdown CHOP expression, A549 cells were seeded in six-well plates and cultured for 24 h. siRNA duplexes against human CHOP (100 nM) or non-targeting control were transfected using Lipofectamine 3000 (Invitrogen, CA, USA) according to the manufacturer's instructions. After 6–8 h, the medium was replaced with fresh medium and cells were cultured for an additional 36 h. Then, cells were treated with NB for 8 h and used for subsequent experiments. CHOP (5′-GCCUGGUAUGAGGACCUGC-3′) and control siRNA (5′-GCGCGCUUUGUAGGAUUCG-3′) were used in this study purchased from GenePharma (Shanghai, China).

In VivoXenograft Model

All animal experiments complied with the Taizhou University's Policy on the Care and Use of Laboratory Animals. Animal studies conducted are in compliance with the ARRIVE guidelines [31]. Nude mice (nu/nu, male, 6–8 weeks old) were purchased from SLAC Laboratories (Shanghai, China). Throughout the experiment, mice were kept in a constant room temperature with a 12/12 h light/dark cycle and fed a standard rodent diet with unlimited access to water. Then, mice were randomly divided into two experimental groups ($n=5$). A549 cells were injected subcutaneously into the right flank of all mice at 5×10^6 cells in 100-μL PBS. After tumor volumes reached 100 mm^3, mice were treated once every 2 days for 18 days with intraperitoneal (i.p.) injections of 5 mg/kg nimbolide (in PBS containing 6% castor oil). A control group of mice received vehicle alone. The tumor volumes were acquired by measuring length (l) and width (w) and calculating volume ($V=0.5\times l\times w^2$) during each of the indicated time points. Mice were sacrificed and tumor specimens were harvested and weighed. The samples were then processed for Western blot and histological analysis.

Tissue Staining

We used 10% formalin to fix harvested tumor tissues and embedded in paraffin. Specimens were sectioned at 5-μm thickness. Tumor sections were stained using routine immunohistochemical techniques with primarily antibodies against cleaved caspase-3 (1:150), p-EIF2α (1:150), γ-H2AX (1:200), or ki-67 (1:200). HRP-conjugated secondary antibodies and diaminobenzidine (DAB) were used for detection.

Heart, liver, and kidney tissues from mice were stained with hematoxylin and eosin (H&E).

Frozen tissue sections were used for immunofluorescence detection of ROS. Sections were incubated with DCFH-DA. Slides were counterstained with DAPI and images were captured.

Statistical Analysis

All experiments were repeated at least three times. Data are reported as mean ± SEM. Statistical analysis was performed with GraphPad Prism 6.0 software (GraphPad, San Diego, CA, USA). Student's *t*-test and two-way analysis of variance were employed to analyze the differences between groups. A p value of < 0.05 was considered statistically significant.

Results

Nimbolide Effectively Suppresses Cell Viability in NSCLC Cells

In order to investigate the effects of NB on cell viability, MTT assays were performed on A549 and H1650 exposed to NB for different durations and concentrations. There was a significant decrease in the viability of both A549 and H1650 cells after NB treatment (Fig. 1A). The IC_{50} values of H1650 and A549 cells were at 2.6 μM (24 h), 2.9 μM (24 h) and 1.9 μM (48 h), 2.4 μM (48 h), respectively. Obviously, IC_{50} of both A549 and H1650 cells were decreased over time. Furthermore, we chose human normal cells L02, to analyze the cytotoxic effect of NB with MTT assay. As shown in Supplementary Figure 1, NB is low toxicity on normal cells compared with cancer cells. The anticancer activities of NB were then detected with the colony formation assay. We exposed H1650 and A549 cells with NB in different doses (0.5, 1, and 2 μM) (Fig. 1B), and these results suggested that NB significantly inhibits the growth in a dose-dependent manner in NSCLC cells (Fig. 1C).

Nimbolide Induces Cell Apoptosis in NSCLC Cells

To explore whether NB induces apoptosis in NSCLC cells, we evaluated the cellular apoptosis using cell apoptosis detection kit. A549 and H460 cells were treated with 1, 2.5, and 5 μM NB. With 1 μM dose of NB treatment, apoptotic cells increased from 5.81 to 13.96%. Similar results also occurred when NB treatment was added from 2.5 to 5 μM (Fig. 2A, B). Therefore, NB treatment (1, 2.5, and 5 μM) on A549 and H460 cells resulted in a rise of apoptotic cells. Moreover, A549 and H460 cells treated with NB significantly downregulated the expression of Bcl-2 and upregulated the expression level of Bax (Fig. 2C–F). All these data showed that treatment of NB induces cell apoptosis in NSCLC cells.

Nimbolide Induces ROS-Dependent Apoptosis in NSCLC Cells

ROS generation has been reported to play a vital role in apoptosis progress induced by NB in some cancer cell lines [19, 27, 32]. Thus, we detected the ROS level in NB-treated cells through flow cytometry. As shown in Fig. 3A and B, NB treatment increased ROS levels in A549 cells in a dose-dependent manner. However, when GSH was added, ROS

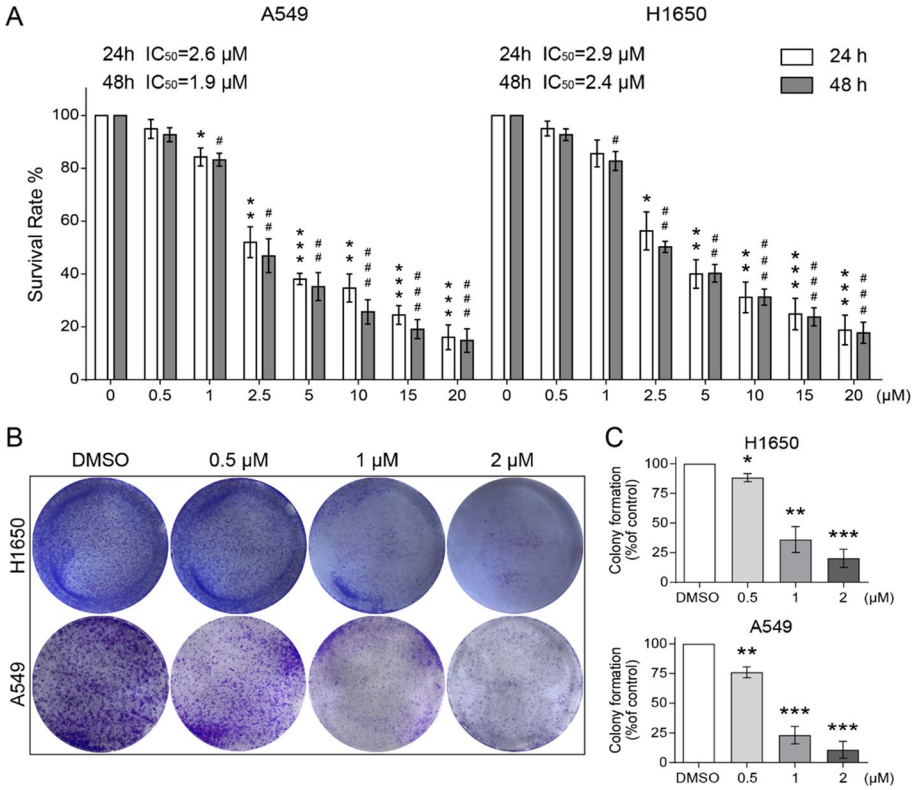

Fig. 1 Nimbolide (NB) inhibits proliferation of NSCLC cells. **A** Cell viability was analyzed by MTT assay. A549 and H1650 cells were treated with different concentrations of NB (0, 0.5, 1, 2.5, 5, 10, 20 μM) for 24 h or 48 h. IC_{50} values for NB were calculated. **B** Colony formation assay. A549 and H1650 cells were incubated with NB (0.5, 1, 2 μM) for a week and stained with crystal violet. Then, the number of colonies was counted. **C** The colony formation ability of each group was shown in bar chart. All data are shown as mean ± SEM ($n = 3$) (*$p < 0.05$, **$p < 0.01$, ***$p < 0.001$; #$p < 0.05$, ##$p < 0.01$, ###$p < 0.001$; all versus DMSO group)

content was decreased (Fig. 3C, D). To investigate whether GSH have inhibitory effect to NB-induced apoptosis, we evaluated the cellular apoptosis by using cell apoptosis analysis. After treated with 5 μM NB, the apoptotic cells remarkedly increased ($P < 0.05$). Interestingly, when pretreatment with GSH (the ROS scavenger), the apoptosis effects induced by NB was significantly reversed (Fig. 3E, F). Moreover, NB treatment downregulated the expression of anti-apoptotic proteins Bcl-2 and upregulated the expression of pro-apoptotic proteins Bax. Pre-incubation of GSH, all these effects were almost attenuated (Fig. 3G, H). All these results suggested that NB induces ROS-mediated cell apoptosis.

Nimbolide Causes ER Stress Activation in NSCLC Cells

Next, we investigated whether NB caused ER stress activation in A549 cells; we used Western blot analysis to measure the protein expression of P-EIF2α, EIF2α, ATF4, and CHOP. All those proteins above were interrelated to ER stress. As shown in Fig. 4A–B,

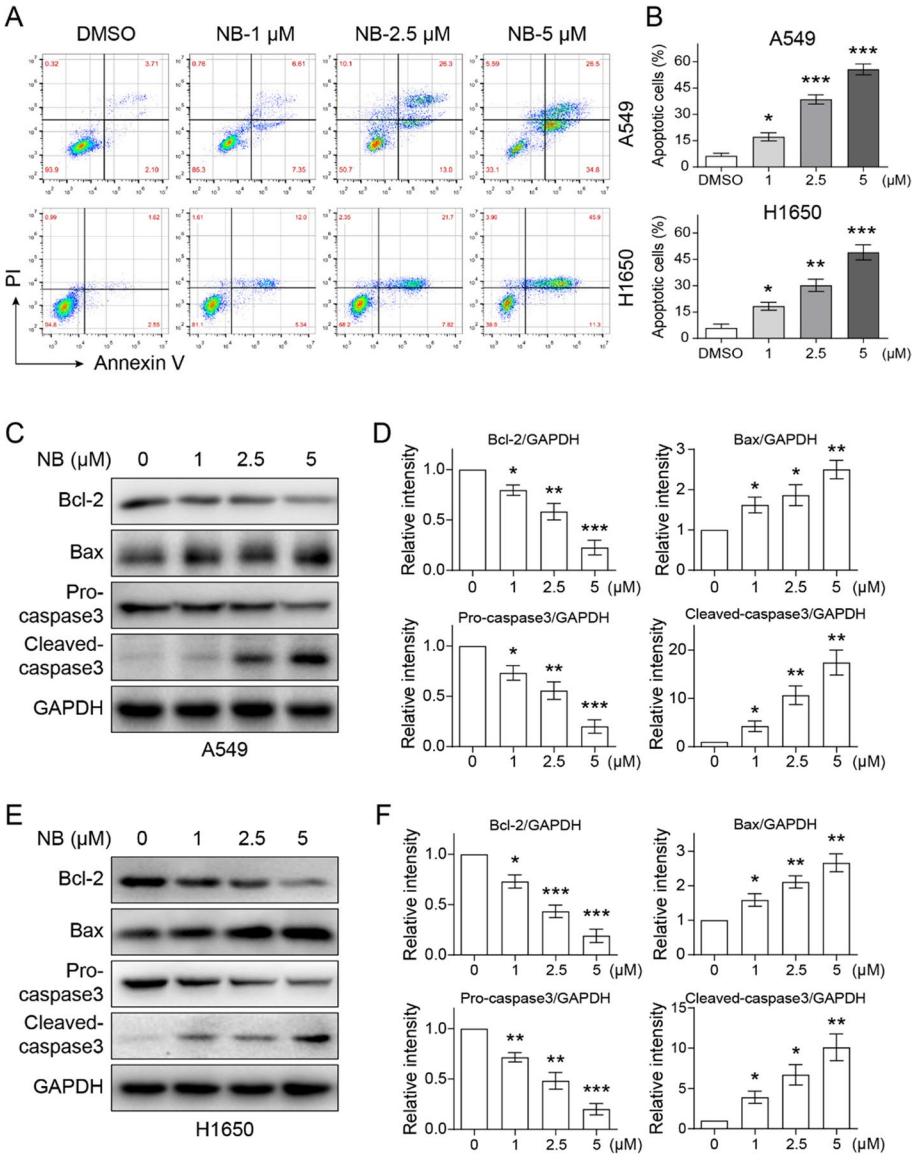

Fig. 2 NB treatment induces apoptosis in NSCLC cells. **A** A549 cells and H1650 cells were exposed to NB at the indicated concentrations (1, 2.5, 5 μM) for 24 h. Percentage of cell apoptosis was determined by Annexin V/PI staining and flow cytometry. Similar results were obtained in three independent experiments. **B** The percentage of apoptotic cells in the treatment groups was quantified. **C**, **E** Expression of apoptosis-related proteins Bcl-2, Bax, pro-caspase-3, and cleaved caspase-3 was determined by Western blot after treatment with NB (1, 2.5, 5 μM) for 20 h in A549 cells and H1650 cells. GAPDH was used as internal control. **D**, **F** Quantification of data presented in (**C**) and (**E**). All data are shown as mean ± SEM ($n = 3$) (*$p < 0.05$, **$p < 0.01$, and ***$p < 0.001$ compared with DMSO)

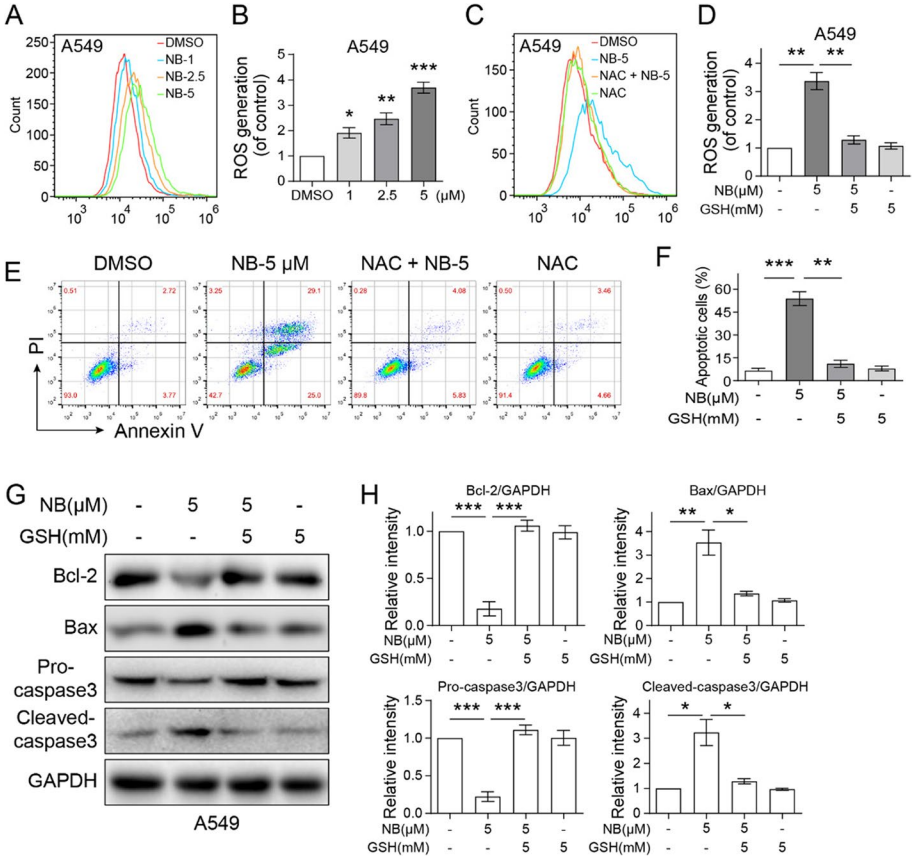

Fig. 3 NB induces ROS accumulation and ROS-dependent apoptosis in NSCLS cells. **A** Intracellular ROS generation dose-dependently induced by NB was measured in A549 cells by staining with DCFH-DA (10 μM) and flow cytometry analysis. A549 cells were treated with NB at the indicated concentrations (1, 2.5, 5 μM) for 3 h. Then, intracellular ROS generation was measured by flow cytometry. **B** Quantification of data presented in (**A**). **C** Effect of GSH pretreatment of 2 h on ROS levels. Relative fluorescence intensity was assayed by flow cytometer. **D** Quantification of data presented in (C). **E** A549 cells were pre-incubated with or without 5 mM GSH for 2 h before exposure to NB (5 μM) for 24 h. Percentage of cell apoptosis was determined by Annexin V/PI staining and flow cytometry. **F** The percentage of apoptotic cells in the treatment groups was quantified. **G** Expression of apoptosis-related proteins Bcl-2, Bax, pro-caspase-3, and cleaved caspase-3 was determined by Western blot after treatment with NB (5 μM) or NB (5 μM) + GSH (5 mM) pretreated or GSH (5 mM) for 20 h in A549 cells. GAPDH was used as internal control. **H** Quantification of data presented in (**G**). All data are shown as mean ± SEM ($n = 3$) (*$p < 0.05$, **$p < 0.01$, and ***$p < 0.001$)

A549 cells were treated with NB (1, 2.5, 5 μM) for 3 h; the expression level of P-EIF2α and ATF4 was upregulated. Besides, the expression of CHOP was also upregulated with NB treatment for 8 h (Fig. 4C). Furthermore, while the dose of NB was increased, relative mRNA intensity of ATF4 and CHOP positively was increased (Fig. 4D). These results demonstrated that NB has an influence to ER-related proteins that causes ER stress activation in A549 cells.

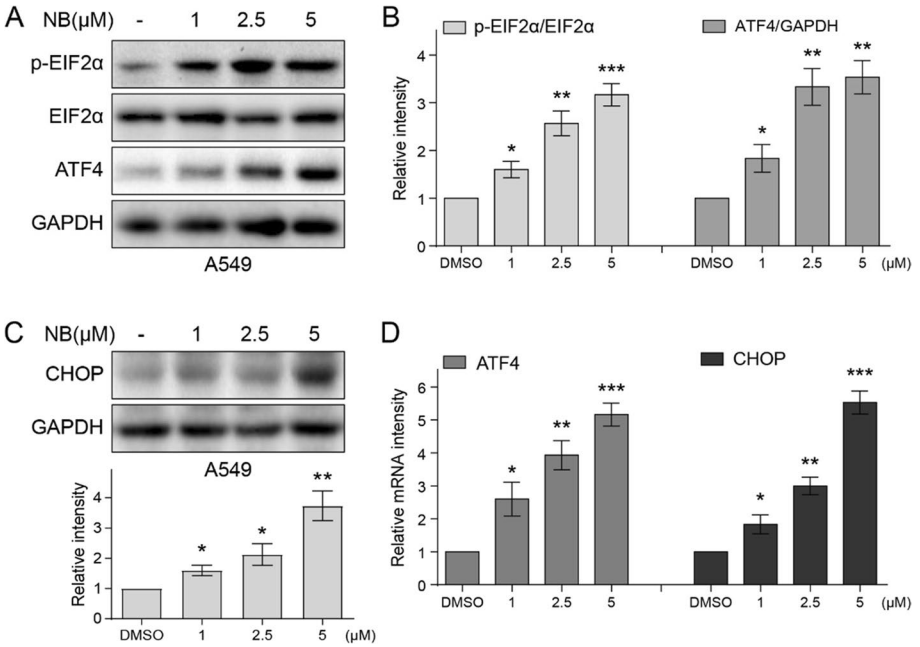

Fig. 4 NB treatment activates ER stress pathway in NSCLS cells. **A** Western blot analysis of ER stress pathway-associated proteins in A549 cells exposed to various concentrations of NB (1, 25, 5 μM) for 3 h (ATF-4 and p-EIF2α). EIF2α and GAPDH served as controls. **B** Quantification of data presented in (**A**). **C** A549 cells were treated with various concentrations of NB (1, 25, 5 μM) for 8 h (CHOP). GAPDH served as controls. **D** Quantification of data presented in (**C**). **E** A549 cells were treated with NB (1, 25, 5 μM) for 3 h or 8 h. The mRNA expression of AFT4 and CHOP was analyzed by qRT-PCR. All data are shown as mean ± SEM ($n = 3$) (*$p < 0.05$, **$p < 0.01$, and ***$p < 0.001$ compared with DMSO group)

Induction of ER Stress by Nimbolide Is Dependent on ROS Generation in NSCLC Cells

Previous research has indicated that ROS generation plays an important role in cell apoptosis and can be used as anticancer agents [33–36]. Thus, we examined whether ROS generation is necessary for NB-induced ER stress in A549 cells. The ER stress relative protein expression of P-EIF2α, ATF4, and CHOP was highly increased when treated with 5 μM NB. Interestingly, pretreatment of GSH almost reversed the above effect induced by NB (Fig. 5A–D). Furthermore, we found that NB treatment contributed to a remarkably increasing in the mRNA levels of ATF4 and CHOP (Fig. 5E, F). Our further study investigated whether ER stress induced by NB was involved in the cell apoptosis process. Thus, the effect of siRNA-mediated CHOP knockdown was further observed in A549 cells. As was described in Fig. 5G–I, protein levels and relative mRNA intensity significantly decreased via 5 μM NB treatment combined with transfection of CHOP siRNA. We therefore assumed that if ER stress was involved in cell death after NB treatment, the apoptosis effect would be reversed after knockdown of CHOP. As shown in Fig. 5J, CHOP knockdown significantly decreased cell apoptosis after NB treatment. These results indicated that NB induced ER stress via ROS generation, eventually leading to cell apoptosis in A549 cells.

Fig. 5 NB induces apoptosis through ROS-dependent ER stress pathway in NSCLS cells. **A** Effect of GSH pretreatment on NB-induced ER stress pathway proteins. GSH was used at 5 mM for 2 h before exposure to NB (ATF-4 and p-EIF2α). EIF2α and GAPDH were served as internal controls. **B** Histogram data indicates densitometric quantification of (**A**). **C** A549 cells were treated with various concentrations of NB (1, 25, 5 μM) for 8 h (CHOP) before GSH pretreatment. GAPDH was served as internal controls. **D** Quantification of data presented in (**C**). **E**, **F** A549 cells were treated with NB (1, 25, 5 μM) for 3 h or 8 h before GSH pretreatment. The mRNA expression of AFT4 and CHOP was analyzed by qRT-PCR. **G** A549 cells transfected with CHOP siRNA or control siRNA were treated with NB (5 μM) for 8 h; the protein level of CHOP was determined by Western blot. **H** Quantification of data presented in (**G**). **I** A549 cells were infected with CHOP siRNA or control siRNA; the mRNA expression of CHOP was analyzed by qRT-PCR after treatment with NB (5 μM) for 8 h. **J** A549 cells transfected with CHOP siRNA or control siRNA were treated with NB (5 μM) for 24 h; percentage of cell apoptosis was determined by Annexin V/PI staining and flow cytometry. All data are shown as mean ± SEM ($n = 3$) (*$p < 0.05$, **$p < 0.01$, and ***$p < 0.001$)

Nimbolide Triggers ROS-Mediated DNA Damage and DNA Damage Response in NSCLC Cells

It is shown that the accumulation of unrepaired DNA damage may lead to apoptosis [37]. Moreover, several natural products selectively kill cancer cells via causing oxidative DNA damage. In our study, we detected the effect of NB treatment (20 h) on DNA integrity using the comet assay in A549 cells. As expect, the alkaline comet assays revealed that NB treatment (1.25–5 μM) triggered massive DNA damage, which caused DNA fragments exiting from the genome and formed "tails" with the cell nuclei (Fig. 6A). The abundance of DNA damage-induced fragments was quantified by the percentage of tail DNA (Fig. 6B). Immunofluorescence (IF) analysis showed that the number of nuclear 53BP1 foci was obviously increased after NB treatment in A549 cells (Fig. 6C). Besides, NB treatment significantly increased γ-H2AX expression level, a marker of DNA double-strand break (Fig. 6D, E). ROS is a DNA damage factor [38]. Therefore, we validated that DNA damage caused by NB is associated with ROS production. Results showed that GSH significantly reduced the accumulation of tail DNA by inhibiting ROS production (Fig. 6F, G). Moreover, pretreatment of GSH significantly attenuated the formation of 53BP1 nuclear foci in A549 cells (Fig. 6H). The results were consistent with the Western blot analysis, which showed that ROS inhibition observably reduced the expression of γ-H2AX (Fig. 6I, J). Together, all data revealed that NB induced cell apoptosis via triggering massive DNA damage as well as strong DNA damage responses.

Nimbolide Inhibits A549 Xenograft Tumor Growth In Vivo

We next investigated the anti-tumor effect of nimbolide in vivo; we subcutaneously implanted A549 cells into immunodeficient mice and orally treated the mice with NB. Treatment of mice with NB (5 mg/kg) reduced NSCLC growth, as evidenced by lower tumor volumes and reduced weights (Fig. 7A–C). Besides, mice treated with NB were seen without any changes to body weight measurements compared to vehicle group (Fig. 7D).

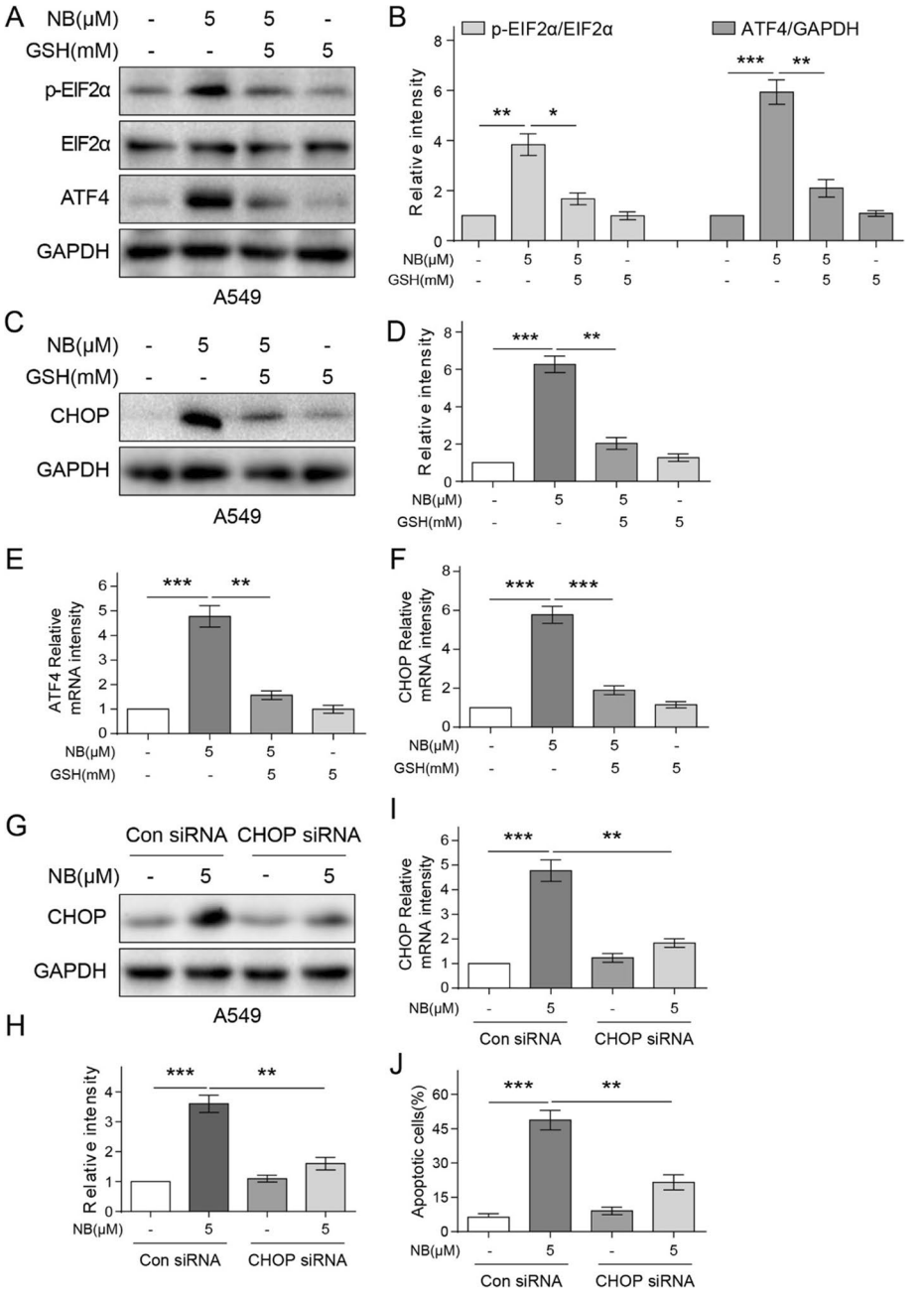
A
NB(μM) - 5 5 -
GSH(mM) - - 5 5
p-EIF2α
EIF2α
ATF4
GAPDH
A549
B
p-EIF2α/EIF2α
ATF4/GAPDH
Relative intensity
C
CHOP
D
E
ATF4 Relative mRNA intensity
F
CHOP Relative mRNA intensity
G
Con siRNA
CHOP siRNA
H
I
J
Apoptotic cells(%)

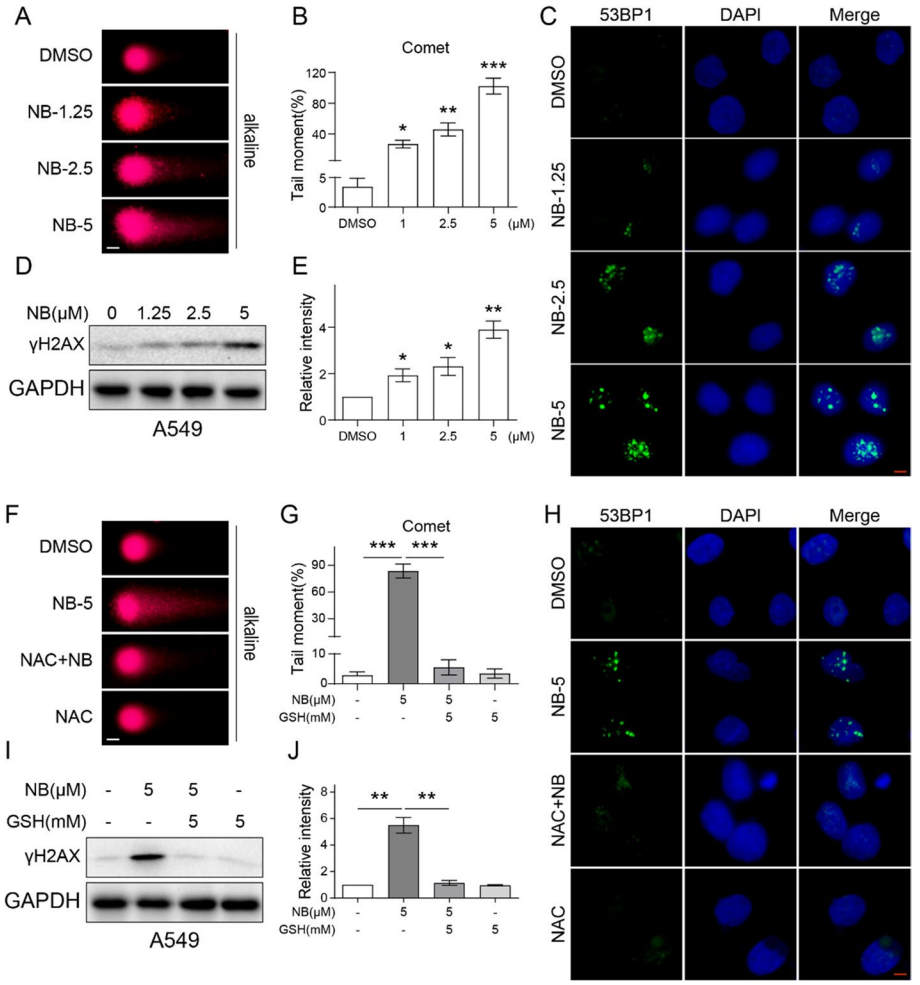

Fig. 6 NB triggered DNA damage and DNA damage response in NSCLC cells. **A** The alkaline comet assay was carried out to assess DNA damage in A549 cells. Scale bar, 10 μm. **B** Quantification of the results shown in **A**. Data are shown as mean ± SEM ($n = 3$) (*$p < 0.05$, **$p < 0.01$, ***$p < 0.001$ compared with DMSO group). **C** The accumulation of 53BP1 (green) nuclear foci as a marker of the DNA damage response was evaluated by immunofluorescence (IF). Nuclei were stained with DAPI (blue). Scale bar, 10 μm. **D**, **E** A549 cells were exposed to NB for 20 h, and the protein level of γ-H2AX, a DNA damage response marker, was determined by Western blot analysis. GAPDH was used as a loading control. Quantification of the results shown in (**E**). **F**–**H** A549 cells were pretreated with 5 mM GSH for 2 h before exposure to NB for 20 h. The alkaline comet assay was performed to detect DNA damage in (**F**). Quantification of tail DNA was shown in (**G**). The nuclear foci formation of 53BPl was detected by immunofluorescence staining in (**H**). Scale bar, 10 μm. **I**, **J** A549 cells were pretreated with 5 mM GSH for 2 h before exposure to NB for 20 h. The protein level of γ-H2AX was determined by Western blot analysis. GAPDH was used as a loading control. Quantification of the results shown in (**J**). All data are shown as mean ± SEM ($n = 3$). (*$p < 0.05$, **$p < 0.01$, and ***$p < 0.001$)

Furthermore, Hematoxylin and Eosin (H&E) staining showed that NB treatment did not induce noticeable histological changes in liver, kidney and heart tissues compared to vehicle group (Fig. 7E). Additionally, we stained tissue sections with DCFH-DA probe to assess ROS levels in tumor specimens. Our data showed that NB treatment increases DCF fluorescence in tumor specimens, indicating increased ROS levels (Fig. 7F). Western blot analysis revealed that treatment with NB significantly increased the expression level of Bax and decreased the expression of Bcl-2 in resected tumor specimens (Fig. 7G). In the xenograft tumors, IHC staining assay was employed to assess the protein expression of representative tumor progression, ER stress, DNA damage, and apoptosis markers. The results showed that Ki-67 expression was decreased after NB-treated group compared to vehicle group, while the p-EIF2α, γ-H2AX, and cleaved caspase-3 expression were increased (Fig. 7H). Taken together, our in vivo findings indicate that NB inhibits tumor growth via triggering ROS production, ER stress, DNA damage, and apoptosis.

Discussion

The aim of our study is to clarify the anticancer molecular mechanisms of NB in NSCLC cells. There is sufficient evidence that NB inhibits cell growth and leads to apoptosis of NSCLC cells. Furthermore, NB treatment caused an increase in ROS production in A549 cells, which leads to the activation of ER stress and DNA damage. Moreover, pretreatment of GSH (a selective inhibitor of ROS) notably reversed NB-induced ER stress and DNA damage, which eventually inhibiting cell apoptosis. Importantly, knockdown of the key protein CHOP in ER stress process by siRNA almost attenuated the apoptosis effect induced by NB. This anti-tumor activity in vivo was also mediated by enhancing ROS levels. Our study shows a novel mechanism of the NSCLC cells apoptosis-inducing activity of NB (summarized in Fig. 8).

Due to the advancements in diagnostics, the 10-year survival rate for NSCLC has increased over the past three decades [5, 39, 40]. However, effective interventions such as surgery and chemotherapy do not guarantee a cure for NSCLC patients, especially those who resist to accept therapeutic regimen. Besides, treatment options for NSCLC currently are presently unsatisfactory, since hormonal resistance is virtually inevitability, and is the leading cause of death [41]. Thus, it is urgent to search for natural compounds with properties of less toxic and anticancer to treat tumor diseases.

There is a complex relationship between ROS and cancer. ROS including hydrogen peroxide (H2O2), super anions ($O2^{-}$), and hydroxyl radical (·OH) are produced as byproducts of cellular metabolism and are in a cellular redox balance with biochemical antioxidants [42]. Unfortunately, in many cancers such as lung cancer, the disruption of this important balance leads to oxidative stress, leading to the formation of ROS, which can damage DNA, RNA, and some proteins and cause some human diseases such as some malignant tumor and insulin-resistant diabetes mellitus [43]. When DNA is damaged, the double-strand break (DSB) can lead to rapid phosphorylation of H2AX (γ-H2AX) which forms foci around the site to keep chromatin open and to provide a platform for the follow-up response to DNA damage. Tumor protein p53 binding protein 1 (53BP1), which is also indicative of DNA double-strand breaks, is upregulated by ATM and ATR [44].

Fig. 7 NB inhibits the growth of A549 xenografts by inducing oxidative stress. **A** A549 cells were implanted in nude mice. Mice were then treated with NB for 18 days. Photographs of resected tumor tissues from mice. **B** Weights of tumor tissues resected from nude mice at the end of the treatment period (**$p < 0.01$ compared to Ctrl group). **C** Measurement of tumor volumes at indicated time points following NB treatment (**$p < 0.01$ compared to Ctrl group). **D** Body weights of nude mice receiving NB treatment at various intervals. **E** HE staining of the major organs including the liver, kidney, and heart (scale bar = 50 μm). **F** Staining of tumor tissue sections for DCFH-DA (green). Tissues were counterstained with DAPI (blue). Increased fluorescence intensity is indicative of increased ROS levels (scale bar = 100 μm). **G** Western blot analysis of Bcl-2 and BAX levels in resected tumor tissues. GAPDH was used as loading control (**$p < 0.01$ compared to Ctrl group). **H** Immunohistochemistry staining was performed to detect the expression of Ki-67, p-EIF2α, γ-H2AX, and cleaved caspase-3 after treatment with NB (scale bar = 50 μm)

In the present study, NB significantly increased γ-H2AX and 53BP1 in a dose-dependent manner. Pretreatment of GSH markedly inhibits NB-induced DNA damage marker. Based on our results, we conclude that treatment of NB resulted in a classic DNA damage. These findings provide evidence for the use of NB, a ROS modulator and DNA damage inducer, in the treatment of NSCLC.

ER stress is essential organelle in protein folding secretion and modification [45]. It has recently been shown that many natural products, such as licochalcone A, chaetocin, and emodin, could induce ER stress-mediated apoptosis in lung cancer cells [46, 47]. When ER stress occurred, unfolding proteins such as ATF4 and p-EIF2α accumulated which triggered the unfolded proteins response. As previously mentioned, cancer cells treated with NB exhibited an increase in ER stress-related protein expression. Western blot data showed that NB treatment observably increased the expression of the ATF4, CHOP, and p-EIF2α in a dose-dependent manner. Research also showed that ROS plays an essential role in IBC-induced ER stress pathway in PC-3 cells [33]. Consistent with above studies, pretreatment with GSH obviously inhibited NB-induced ER stress relative protein overexpression. We also found that NB treatment led to a great increasing of relative mRNA level of CHOP and ATF4. All these results indicated that NB selectively activates ER stress which can be influenced by ROS and exhibited excellent anticancer activities in A549 cells. Besides, our results demonstrated that the ROS generation has a substantial influence to apoptosis and it can serve as anticancer strategy and inhibit the development of some tumor diseases.

Conclusion

In summary, our present study showed that NB inhibits cancer cell growth and apoptosis via ROS-mediated ER stress and DNA damage in vitro and in vivo. It provides a potential therapeutic agent (NB) for treating NSCLC. Besides, our results also indicate that targeting ROS-mediated ER stress and DNA damage is a key step in developing anti-NSCLC drugs.

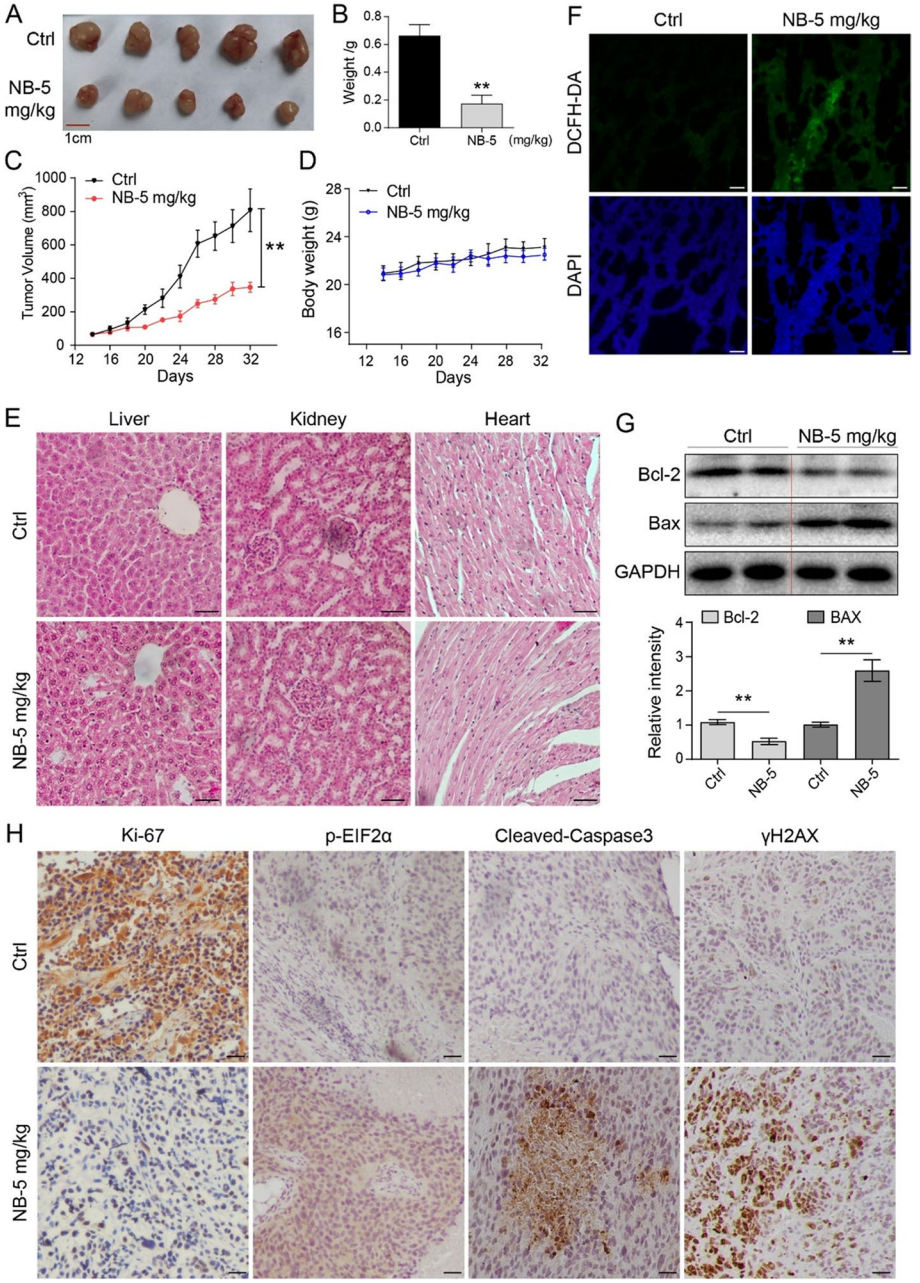
A
Ctrl
NB-5 mg/kg
1cm
B
Weight /g
0.8
0.6
0.4
0.2
0.0
**
Ctrl
NB-5
(mg/kg)
C
Tumor Volume (mm³)
1000
800
600
400
200
0
Ctrl
NB-5 mg/kg
**
12 16 20 24 28 32
Days
D
Body weight (g)
28
24
20
16
Ctrl
NB-5 mg/kg
12 16 20 24 28 32
Days
F
Ctrl
NB-5 mg/kg
DCFH-DA
DAPI
E
Liver
Kidney
Heart
Ctrl
NB-5 mg/kg
G
Ctrl
NB-5 mg/kg
Bcl-2
Bax
GAPDH
Bcl-2
BAX
Relative intensity
4
3
2
1
0
**
**
Ctrl
NB-5
Ctrl
NB-5
H
Ki-67
p-EIF2α
Cleaved-Caspase3
γH2AX
Ctrl
NB-5 mg/kg

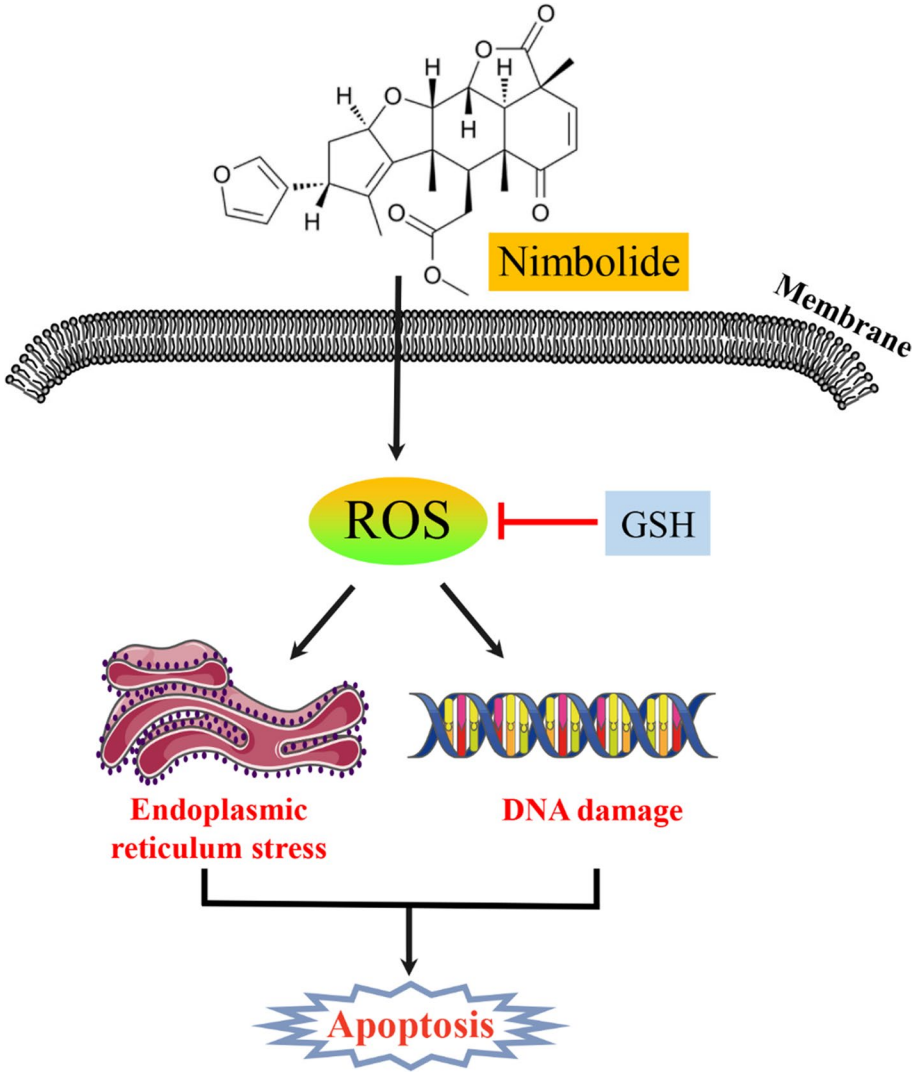

Fig. 8 Schematic illustration of the ROS-ER stress/DNA damage signaling axis in nimbolide-induced apoptosis in NSCLC cells

Supplementary Information The online version contains supplementary material available at https://doi.org/10.1007/s12010-023-04507-9.

Author Contribution This work was carried out in collaboration among all authors. X C, JB W, and N Z contributed to the literature search and study design. X C, JB W, and G C participated in the drafting of the article. X C, N Z, HS Z, and YZ P carried out the experiments. JB W and LS Z revised the manuscript. IB W, HS Z, and YZ P contributed to data collection and analysis. All authors have read and approved the final manuscript.

Funding This study was supported by the Medical Health Science and Technology Project of Zhejiang Provincial Health Commission (No. 2021KY399) and the Science and Technology Plan Project of Taizhou (No. 22ywb83).

Data Availability Not applicable.

Declarations

Ethical Approval Permission from the Institutional Animal Ethical Committee was received before making these experiments.

Consent to Participate All authors have their consent to participate.

Consent for Publication All authors have their consent to publish their work.

Conflict of Interest The authors declare no competing interests.

References

1. Bray, F., Ferlay, J., Soerjomataram, I., Siegel, R. L., Torre, L. A., & Jemal, A. (2018). Global cancer statistics 2018: GLOBOCAN estimates of incidence and mortality worldwide for 36 cancers in 185 countries. *CA: A Cancer Journal for Clinicians, 68*(6), 394–424.
2. Siegel, R., Naishadham, D., & Jemal, A. (2013). Cancer statistics, 2013. *CA: A Cancer Journal for Clinicians, 63*(1), 11–30.
3. Sakashita, S., Sakashita, M., & Sound Tsao, M. (2014). Genes and pathology of non-small cell lung carcinoma. *Seminars in Oncology, 41*(1), 28–39.
4. Vyfhuis, M. A. L., Mohindra, P., & Simone, C. B. (2019). Stereotactic body radiation therapy versus thermal ablation for early stage non-small cell lung cancer. *Radiology, 290*(2), 574–575.
5. Stinchcombe, T. E., Fried, D., Morris, D. E., & Socinski, M. A. (2006). Combined modality therapy for stage III non-small cell lung cancer. *The Oncologist, 11*(7), 809–823.
6. Zhang, J., Yu, J., Sun, X., & Meng, X. (2014). Epidermal growth factor receptor tyrosine kinase inhibitors in the treatment of central nerve system metastases from non-small cell lung cancer. *Cancer Letters, 351*(1), 6–12.
7. Katanasaka, Y., Kodera, Y., Yunokawa, M., Kitamura, Y., Tamura, T., & Koizumi, F. (2014). Synergistic anti-tumor effects of a novel phosphatidyl inositol-3 kinase/mammalian target of rapamycin dual inhibitor BGT226 and gefitinib in non-small cell lung cancer cell lines. *Cancer letters, 347*(2), 196–203.
8. (2018). Osimertinib treats CNS metastases in NSCLC. *Cancer discovery, 8*(11), Of3
9. Lee, C. K., Davies, L., Wu, Y. L., Mitsudomi, T., Inoue, A., Rosell, R., Zhou, C., Nakagawa, K., Thongprasert, S., Fukuoka, M., Lord, S., Marschner, I., Tu, Y. K., Gralla, R. J., Gebski, V., Mok, T. & Yang, J. C. (2017). Gefitinib or erlotinib vs chemotherapy for EGFR mutation-positive lung cancer: Individual patient data meta-analysis of overall survival. *Journal of the National Cancer Institute, 109*(6)
10. Zhou, C., Wu, Y. L., Chen, G., Feng, J., Liu, X. Q., Wang, C., Zhang, S., Wang, J., Zhou, S., Ren, S., Lu, S., Zhang, L., Hu, C., Hu, C., Luo, Y., Chen, L., Ye, M., Huang, J., Zhi, X., … You, C. (2011). Erlotinib versus chemotherapy as first-line treatment for patients with advanced EGFR mutation-positive non-small-cell lung cancer (OPTIMAL, CTONG-0802): A multicentre, open-label, randomised, phase 3 study. *The Lancet Oncology, 12*(8), 735–742.
11. Mitsudomi, T., Morita, S., Yatabe, Y., Negoro, S., Okamoto, I., Tsurutani, J., Seto, T., Satouchi, M., Tada, H., Hirashima, T., Asami, K., Katakami, N., Takada, M., Yoshioka, H., Shibata, K., Kudoh, S., Shimizu, E., Saito, H., Toyooka, S., … West Japan Oncology, Group. (2010). Gefitinib versus cisplatin plus docetaxel in patients with non-small-cell lung cancer harbouring mutations of the epidermal growth factor receptor (WJTOG3405): An open label, randomised phase 3 trial. *The Lancet Oncology, 11*(2), 121–128.
12. Maemondo, M., Inoue, A., Kobayashi, K., Sugawara, S., Oizumi, S., Isobe, H., Gemma, A., Harada, M., Yoshizawa, H., Kinoshita, I., Fujita, Y., Okinaga, S., Hirano, H., Yoshimori, K., Harada, T., Ogura, T., Ando, M., Miyazawa, H., Tanaka, T., … North-East Japan Study, Group. (2010). Gefitinib or chemotherapy for non-small-cell lung cancer with mutated EGFR. *New England Journal of Medicine, 362*(25), 2380–2388.
13. D'Autréaux, B., & Toledano, M. B. (2007). ROS as signalling molecules: Mechanisms that generate specificity in ROS homeostasis. *Nature Reviews Molecular cell biology, 8*(10), 813–824.

14. Raza, M. H., Siraj, S., Arshad, A., Waheed, U., Aldakheel, F., Alduraywish, S., & Arshad, M. (2017). ROS-modulated therapeutic approaches in cancer treatment. *Journal of Cancer Research and Clinical Oncology, 143*(9), 1789–1809.
15. Metallo, C. M., & Vander Heiden, M. G. (2013). Understanding metabolic regulation and its influence on cell physiology. *Molecular Cell, 49*(3), 388–398.
16. Cragg, G. M., Grothaus, P. G., & Newman, D. J. (2009). Impact of natural products on developing new anti-cancer agents. *Chemical Reviews, 109*(7), 3012–3043.
17. Seo, J. Y., Lee, C., Hwang, S. W., Chun, J., Im, J. P., & Kim, J. S. (2016). Nimbolide inhibits nuclear factor-capital KA, CyrillicB pathway in intestinal epithelial cells and macrophages and alleviates experimental colitis in mice. *Phytotherapy Research : PTR, 30*(10), 1605–1614.
18. Gupta, S. C., Prasad, S., Sethumadhavan, D. R., Nair, M. S., Mo, Y. Y., & Aggarwal, B. B. (2013). Nimbolide, a limonoid triterpene, inhibits growth of human colorectal cancer xenografts by suppressing the proinflammatory microenvironment. *Clinical Cancer Research : An Official Journal of the American Association for Cancer Research, 19*(16), 4465–4476.
19. Zhang, J., Ahn, K. S., Kim, C., Shanmugam, M. K., Siveen, K. S., Arfuso, F., Samym, R. P., Deivasigamanim, A., Lim, L. H., Wang, L., Goh, B. C., Kumar, A. P., Hui, K. M., & Sethi, G. (2016). Nimbolide-induced oxidative stress abrogates STAT3 signaling cascade and inhibits tumor growth in transgenic adenocarcinoma of mouse prostate model. *Antioxidants & Redox Signaling, 24*(11), 575–589.
20. Sarkar, P., Acharyya, S., Banerjee, A., Patra, A., Thankamani, K., Koley, H., & Bag, P. K. (2016). Intracellular, biofilm-inhibitory and membrane-damaging activities of nimbolide isolated from Azadirachta indica A. Juss (Meliaceae) against meticillin-resistant Staphylococcus aureus. *Journal of Medical Microbiology, 65*(10), 1205–1214.
21 Lin, H., Qiu, S., Xie, L., Liu, C., & Sun, S. (2017). Nimbolide suppresses non-small cell lung cancer cell invasion and migration via manipulation of DUSP4 expression and ERK1/2 signaling. *Biomedicine & Pharmacotherapy= Biomedecine & Pharmacotherapie, 92*, 340–346.
22. Babykutty, S., Priya, P. S., Nandini, R. J., Kumar, M. A., Suresh, N., Mangalam, S., Srinivas, P., & Gopala, S. (2012). Nimbolide retards tumor cell migration, invasion, and angiogenesis by downregulating MMP-2/9 expression via inhibiting ERK1/2 and reducing DNA-binding activity of NF-κB in colon cancer cells †. *Molecular Carcinogenesis, 51*(6), 475–490.
23. Elumalai, P., Gunadharini, D. N., Senthilkumar, K., Banudevi, S., Arunkumar, R., Benson, C. S., Sharmila, G., & Arunakaran, J. (2012). Induction of apoptosis in human breast cancer cells by nimbolide through extrinsic and intrinsic pathway. *Toxicology Letters, 215*(2), 131–142.
24. Hsueh, K. C., Lin, C. L., Tung, J. N., Yang, S. F., & Hsieh, Y. H. (2018). Nimbolide induced apoptosis by activating ERK-mediated inhibition of c-IAP1 expression in human hepatocellular carcinoma cells. *Environmental Toxicology, 33*(9), 913–922.
25. Pooladanda, V., Bandi, S., Mondi, S. R., Gottumukkala, K. M., & Godugu, C. (2018). Nimbolide epigenetically regulates autophagy and apoptosis in breast cancer. *Toxicology in Vitro, 51*, 114–128.
26. Kumar, S., Inigo, J. R., Kumar, R., Chaudhary, A. K., O'Malley, J., Balachandar, S., Wang, J., Attwood, K., Yadav, N., Hochwald, S., Wang, X., & Chandra, D. (2018). Nimbolide reduces CD44 positive cell population and induces mitochondrial apoptosis in pancreatic cancer cells. *Cancer Letters, 413*, 82–93.
27. Liu, J. F., Hou, C. H., Lin, F. L., Tsao, Y. T., & Hou, S. M. (2015). Nimbolide Induces ROS-regulated apoptosis and inhibits cell migration in osteosarcoma. *International Journal of Molecular Sciences, 16*(10), 23405–23424.
28. Chen, X., Wu, Q., Chen, Y., Zhang, J., Li, H., Yang, Z., Yang, Y., Deng, Y., Zhang, L. & Liu, B. (2019). Diosmetin induces apoptosis and enhances the chemotherapeutic efficacy of paclitaxel in non-small cell lung cancer cells via Nrf2 inhibition. *British Journal of Pharmacology, 176*(12):2079–2094.
29. Olive, P. L., & Banáth, J. P. (2006). The comet assay: A method to measure DNA damage in individual cells. *Nature Protocols, 1*(1), 23–29.
30. Kumar, A., Singh, K. P., Bali, P., Anwar, S., Kaul, A., Singh, O. P., Gupta, B. K., Kumari, N., Noor Alam, M., Raziuddin, M., Sinha, M. P., Gourinath, S., Sharma, A. K., & Sohail, M. (2018). iNOS polymorphism modulates iNOS/NO expression via impaired antioxidant and ROS content in P. vivax and P. falciparum infection. *Redox Biology, 15*, 192–206.
31. McGrath, J. C., & Lilley, E. (2015). Implementing guidelines on reporting research using animals (ARRIVE etc.): New requirements for publication in BJP. *British Journal of Pharmacology, 172*(13), 3189–3193.
32. Subramani, R., Gonzalez, E., Arumugam, A., Nandy, S., Gonzalez, V., Medel, J., Camacho, F., Ortega, A., Bonkoungou, S., Narayan, M., Dwivedi, Ak., & Lakshmanaswamy, R. (2016).

Nimbolide inhibits pancreatic cancer growth and metastasis through ROS-mediated apoptosis and inhibition of epithelial-to-mesenchymal transition. *Science and Reports, 6*, 19819.
33. Malik, F., Kumar, A., Bhushan, S., Khan, S., Bhatia, A., Suri, K. A., Qazi, G. N., & Singh, J. (2007). Reactive oxygen species generation and mitochondrial dysfunction in the apoptotic cell death of human myeloid leukemia HL-60 cells by a dietary compound withaferin A with concomitant protection by N-acetyl cysteine. *Apoptosis : An International Journal on Programmed Cell Death, 12*(11), 2115–2133.
34. Oliveira, M. S., Barbosa, M. I. F., de Souza, T. B., Moreira, D. R. M., Martins, F. T., Villarreal, W., Machado, R. P., Doriguetto, A. C., Soares, M. B. P., & Bezerra, D. P. (2019). A novel platinum complex containing a piplartine derivative exhibits enhanced cytotoxicity, causes oxidative stress and triggers apoptotic cell death by ERK/p38 pathway in human acute promyelocytic leukemia HL-60 cells. *Redox Biology, 20*, 182–194.
35. Zheng, X., Ma, W., Sun, R., Yin, H., Lin, F., Liu, Y., Xu, W., & Zeng, H. (2018). Butaselen prevents hepatocarcinogenesis and progression through inhibiting thioredoxin reductase activity. *Redox Biology, 14*, 237–249.
36. Kim, J., Yun, M., Kim, E. O., Jung, D. B., Won, G., Kim, B., Jung, J. H., & Kim, S. H. (2016). Decursin enhances TRAIL-induced apoptosis through oxidative stress mediated- endoplasmic reticulum stress signalling in non-small cell lung cancers. *British Journal of Pharmacology, 173*(6), 1033–1044.
37. Dolan, D. W., Zupanic, A., Nelson, G., Hall, P., Miwa, S., Kirkwood, T. B., & Shanley, D. P. (2015). Integrated stochastic model of DNA damage repair by non-homologous end joining and p53/p21-mediated early senescence signalling. *PLoS Computational Biology, 11*(5), e1004246.
38. Nunes, S. C. & Serpa, J. (2018). Glutathione in ovarian cancer: A double-edged sword. *International Journal of Molecular Sciences, 19*(7):1882.
39. Li, S., Fan, J., Liu, J., Zhou, J., Ren, Y., Shen, C., & Che, G. (2016). Neoadjuvant therapy and risk of bronchopleural fistula after lung cancer surgery: A systematic meta-analysis of 14 912 patients. *Japanese Journal of Clinical Oncology, 46*(6), 534–546.
40. Scagliotti, G. V., & Novello, S. (2003). Adjuvant therapy in completely resected non-small-cell lung cancer. *Current Oncology Reports, 5*(4), 318–325.
41. Rodriguez-Lara, V., Hernandez-Martinez, J. M., & Arrieta, O. (2018). Influence of estrogen in non-small cell lung cancer and its clinical implications. *Journal of Thoracic Disease, 10*(1), 482–497.
42. Li, K., Zheng, Q., Chen, X., Wang, Y., Wang, D., & Wang, J. (2018). Isobavachalcone induces ROS-mediated apoptosis via targeting thioredoxin reductase 1 in human prostate cancer PC-3 cells. *Oxidative Medicine and Cellular Longevity, 2018*, 1915828.
43. Martin, B. C., Warram, J. H., Krolewski, A. S., Bergman, R. N., Soeldner, J. S., & Kahn, C. R. (1992). Role of glucose and insulin resistance in development of type 2 diabetes mellitus: Results of a 25-year follow-up study. *Lancet, 340*(8825), 925–929.
44. Khanna, K. K., Keating, K. E., Kozlov, S., Scott, S., Gatei, M., Hobson, K., Taya, Y., Gabrielli, B., Chan, D., Lees-Miller, S. P., & Lavin, M. F. (1998). ATM associates with and phosphorylates p53: Mapping the region of interaction. *Nature Genetics, 20*(4), 398–400.
45. Hetz, C. (2012). The unfolded protein response: Controlling cell fate decisions under ER stress and beyond. *Nature Reviews Molecular Cell Biology, 13*(2), 89–102.
46. Chen, G., Ma, Y., Jiang, Z., Feng, Y., Han, Y., Tang, Y., Zhang, J., Ni, H., Li, X., & Li, N. (2018). Lico A causes ER stress and apoptosis via up-regulating miR-144-3p in human lung cancer cell line H292. *Frontiers in Pharmacology, 9*, 837.
47. Liu, X., Guo, S., Liu, X., & Su, L. (2015). Chaetocin induces endoplasmic reticulum stress response and leads to death receptor 5-dependent apoptosis in human non-small cell lung cancer cells. *Apoptosis : An International Journal on Programmed Cell Death, 20*(11), 1499–1507.